High Speed Electron-Beam Dose Modulation by Electrostatic Quadra-Deflection

by

Aleksandr Bernshteyn

Submitted to the Department of Electrical Engineering and Computer Science
in partial fulfillment of the requirements for the degrees of

Bachelor of Science in Electrical Science

and

Master of Engineering in Electrical Engineering and Computer Science

at the

MASSACHUSETTS INSTITUTE OF TECHNOLOGY

May 1999

© Aleksandr Bernshteyn, MCMXCIX. All rights reserved.

The author hereby grants to MIT permission to reproduce and distribute publicly paper and electronic copies of this thesis document in whole or in part.

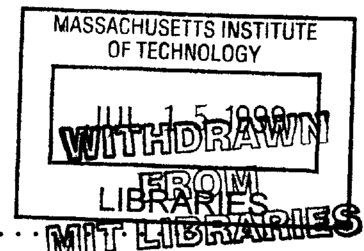

ENG

Author ....
Department of Electrical Engineering and Computer Science
May 21, 1999

Certified by ....
Henry I. Smith
Joseph F & Nancy P Keithley Professor Of Electrical Engineering
Thesis Supervisor

Accepted by ....
Arthur C. Smith
Chairman, Department Committee on Graduate Theses

High Speed Electron-Beam Dose Modulation by Electrostatic Quadra-Deflection

by

Aleksandr Bernshteyn

Submitted to the Department of Electrical Engineering and Computer Science
on May 21, 1999, in partial fulfillment of the
requirements for the degrees of
Bachelor of Science in Electrical Science
and
Master of Engineering in Electrical Engineering and Computer Science

Abstract

Scanning electron beam lithography (SEBL) is capable of writing sub-100-nm features. However, large pattern-placements errors limit its use to lower resolutions. Spatial-phase-locked electron-beam lithography (SPLEBL) greatly improves the pattern-placement precision, thus allowing high fidelity patterns to be written with sub-100-nm features. However, for maximum pattern-placement precision a device is needed that can modulate the intensity of the electron beam by an order of magnitude on a nanosecond time scale. In this thesis, different modulation schemes are discussed, and a quadra electrostatic deflector is proposed as a device that meets the high switching-rate requirement. An analytical description of the electrostatic quadra-deflector is given. Also, an experimental set-up designed to test a prototype device is described, and experimental results are presented.

Thesis Supervisor: Henry I. Smith
Title: Joseph F & Nancy P Keithley Professor Of Electrical Engineering

Acknowledgments

I would like to thank all the people who made the completion of this Master's thesis possible.

First, I would like to thank my research supervisor James Goodberlet. His knowledge and insight were invaluable asset for my research. And his patience in reading and correcting many drafts of this thesis was essential for its successful completion.

I would also like to thank my thesis supervisor Prof. Henry I. Smith for giving me an opportunity to work on this exciting project.

Special thanks go to Katya Doginova, for her constant emotional support and encouragement at times of stress.

Finally, I would like to thank my parents, Tamara and Arnold, for their love and care and for bringing me into the United States thus making my enrollment into MIT possible.

Contents

1 Introduction **11**

1.1 Scanning Electron-Beam Lithography 12

1.1.1 Conventional Round-Beam System 12

1.1.2 Sources of Placement Errors in Scanning-Electron-Beam Lithography 13

1.2 Spatial-Phase-Locked Electron-Beam Litho-graphy 16

1.2.1 Overview of Spatial-Phase-Locked Electron-Beam Lithography 17

1.2.2 Dose-Modulation for Spatial-Phase-Locked Electron-Beam Lithography 17

2 Dose Modulation **21**

2.1 Partial Blanking 21

2.1.1 Magnetic Lenses 21

2.1.2 Conventional Blanker 22

2.2 Controlling Emission 24

2.2.1 Thermionic Emitters 24

2.2.2 Field Emission 24

2.2.3 Photo-cathodes 26

2.2.4 Photo-Assisted Field Emission 26

2.3 Electrostatic Quadra-deflector 26

3 Analytical Description of a Quadra-Deflector **31**

3.1 Static Deflection 32

3.1.1 Transverse Acceleration 32
3.1.2 Deflection at the Aperture Strip 32
3.2 Dynamic Operation 33
3.2.1 Writing Frequency 33
3.2.2 Delay Times 34
3.3 High-Energy Beams 34

4 Experimental Set-up and Results **35**
4.1 Experimental set-up 35
4.1.1 Vacuum System 35
4.1.2 Electron-Optical Rail 35
4.1.3 Electrostatic Einzel Lenses 37
4.1.4 Electron Source 37
4.1.5 Blanking Assembly 37
4.2 Experimental Results 40

5 Conclusion **45**

Bibliography **47**

List of Figures

1-1 Typical Scanning-Electron-Beam-Lithography-System 14

1-2 Spatial-Phase-Locked Electron-Beam Lithography 18

2-1 Use of Magnetic Lenses for Dose Modulation 22

2-2 Image Shift in Conventional Blanking. 23

2-3 Equipotential Lines in a Thermionic Emitter. 25

2-4 Schematic of the Quadra-Deflector 27

2-5 Simulation of the Operation of the Quadra Deflector 28

3-1 Dose Modulator Geometry 32

4-1 Experimental Setup 36

4-2 Tungsten Hairpin Electron Source 38

4-3 Emission Properties of Tungsten Hairpin 39

4-4 Deflector Plates Switching Rate. 41

4-5 Intensity Modulation in a Wide Beam. 43

List of Tables

4.1 Deflector Plate Dimensions 40

Chapter 1

Introduction

According to the Moore's law, the processing power of computers more than doubles every year. Most of this gain can be attributed to the increasing number of transistors that make up computer processors. With advances in lithographic techniques over the recent years, the feature size of electronic components printed on the chip reduced dramatically, thus allowing more transistors, which operate aat increasingly higher speeds, to fit onto a chip.

Most integrated circuits today are produced by means of optical lithography, which involves making multiple copies of a mask on a substrate (typically silicon) covered with a photo-sensitive material. A photo-reduction technique is used so that the patterns on the substrate are one-fifth the size of patterns on the mask. This process is very similar similar to making several prints from a single negative. To achieve high device yields, a high quality mask is essential. As feature sizes continue to decrease, the requirements on mask quality increase significantly. With a potential switch to x-ray lithography in the future, the quality requirements will increase even further since x-ray lithography is a one-to-one imaging scheme.

Masks have been traditionally fabricated with scanning-electron-beam-lithography (SEBL). SEBL is the most effective method of creating patterns of arbitrary geometry on photo-masks and x-ray masks. However, while SEBL is capable of writing very fine patterns, the precision with which those patterns can be placed with respect to each other is very poor. In conventional SEBL systems, the pattern-placement

precision is $3\sigma = 30$ nm to 100 nm which is significantly poorer than the precision required for future sub-100-nm IC lithography. This problem can be overcome with spatial-phase-locked electron-beam lithography (SPLEBL) [6, 7, 11, 12] which can improve the writing precision to $\sigma \leq 2$ nm, about an order of magnitude better than conventional SEBL systems. Unlike conventional SEBL systems, SPLEBL uses a feedback loop to correct pattern-placement errors.

While SPLEBL greatly improves pattern-placement precision, its use is now limited to the fabrication of precise one-dimensional gratings. Several obstacles need to be overcome to use it efficiently for arbitrary two-dimensional patterns and in a wide variety of applications. This work describes the design of a dose modulation system, which is one of the components necessary for the "smooth" operation of a SPLEBL system.

This chapter, Chapter 1, describes principles of operation of SEBL and SPLEBL systems. The need for a dose-modulating blanker is elucidated. Chapter 2 discusses different dose modulation schemes and proposes a new quadra-deflection dose modulator. The physics of operation of the quadra deflector is described in Chapter 3. Chapter 4 describes the experimental system that has been built and provides some experimental results. Finally, Chapter 5, summarizes the most important points of this work.

1.1 Scanning Electron-Beam Lithography

1.1.1 Conventional Round-Beam System

A SEBL system is in essence a scanning-electron microscope, modified to perform lithography (see Fig. 1-1). A demagnified image of a source is produced on the surface of a substrate by a set of lenses. Electrons are extracted from the source and accelerated towards the sample by a potential difference. Magnetic or electric fields produced by special lenses, focus the electron beam to a small spot on the substrate. Applying electric or magnetic field transversely to the trajectory of the beam, shifts

the beam by the amount determined by the magnitude of the field. By means of two orthogonal deflection fields, the beam can be deflected along a Cartesian coordinate system. The beam is blanked by a pair of electrostatic plates that deflect it onto an obstruction, thus preventing it from impinging on the substrate. By integrating all these elements in an electron-optical column, arbitrary patterns can be created on the substrate plane.

The operation of a SEBL system resembles the operation of a CRT. The sample, coated with a material sensitive to electron irradiation, acts as the screen. The beam is turned on and off under computer control, while being scanned in a raster fashion. This allows exposure of any image in a pixel-by-pixel fashion, the same way an image is produced on a CRT screen.

It is not possible to deflect the beam more than several hundred micrometers while keeping it focused on the substrate without causing significant distortions in the pattern. However, masks used in fabrication of modern integrated circuits can be as large as 15 cm. Therefore, large-area patterns are "stitched" together from smaller areas or, so called, fields. This is achieved by fixing the substrate to a movable stage and moving the stage by an appropriate amount between field exposures. The position of the stage is typically measured by a laser interferometer. Modern state-of-the art interferometers boast resolutions of 5 Å in positional accuracy. In principle, it should be possible to place features with this accuracy, but in practice several factors severely restrict the pattern-placement accuracy of a SEBL system.

1.1.2 Sources of Placement Errors in Scanning-Electron-Beam Lithography

There are two classes of pattern-placement errors in a SEBL system:

- Errors that arise from incorrect placement of the substrate with respect to the field produced in the electron beam column. These errorss manifest themselves as abrupt changes in the position of the features at the boundaries between fields and are referred to as **interfield** or **"stitching"** errors.

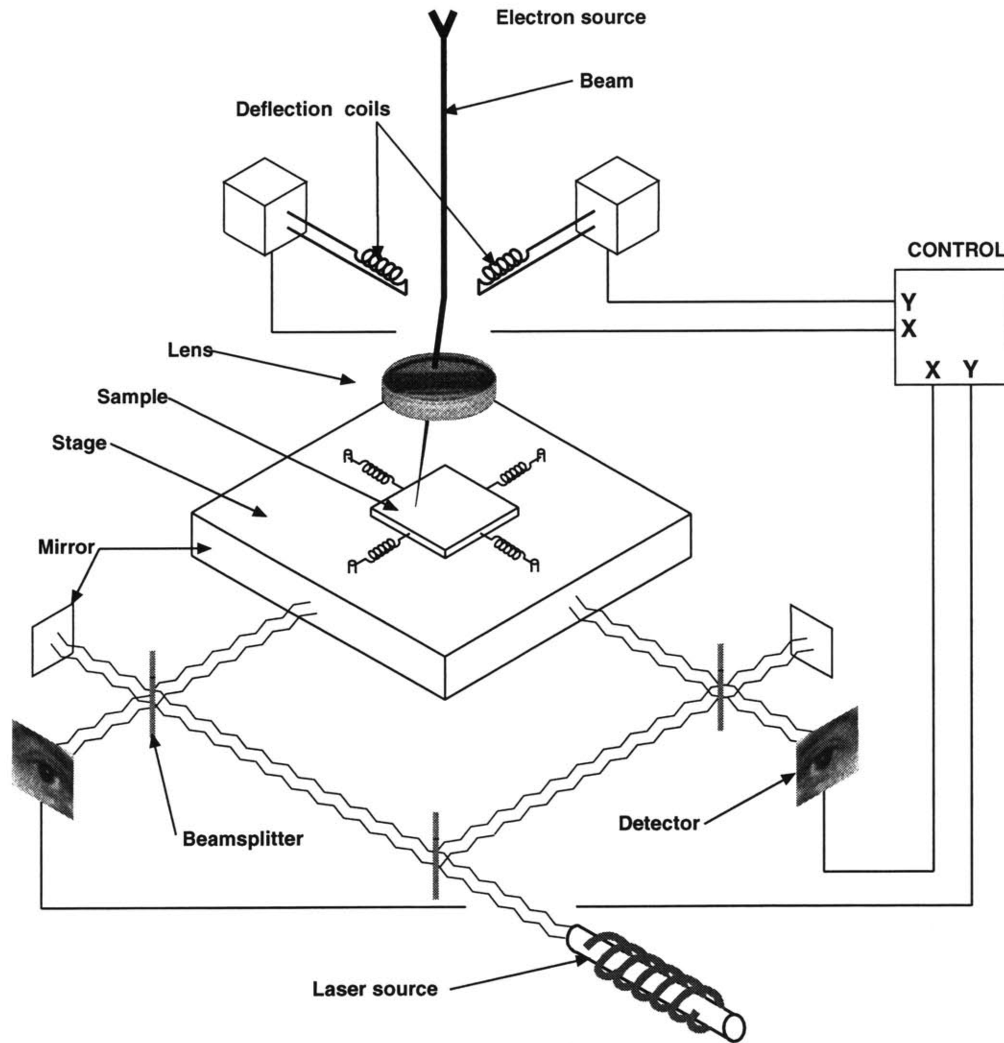

Figure 1-1: Typical Scanning-Electron-Beam-Lithography-System

Figure courtesy of J. Ferrera [6]

- Errors in pattern-placement within a single field or, so called, **intrafield** errors.

Interfield Errors

The sources of interfield errors include [6]:

- Miscalibration of field magnification with respect to the stage coordinate system. If the field size is larger than the distance that separates two fields, as measured by the interferometer, the fields overlap; similarly, if it is smaller, a gap occurs.

- Rotation of field axes with respect to stage motion axes results in gaps and overlaps at different places along the field boundaries. Rotation and magnification can be calibrated to the coordinate system defined by the laser interferometer and, therefore, be made small.

- Errors in the detection of the stage position. Although the stage is designed to move along two perpendicular axes, the movement along other degrees of freedom (z-translation, roll, pitch, and yaw) cannot be completely eliminated. Also, the precision of laser interferometer is limited by flatness of its mirrors. The typical flatness of $\lambda/20$ corresponds to 25 nm precision if 500 nm light is used as reference. Pattern-placement precision cannot be better than the flatness of the mirror, thus making this item a severe limitation for nanometer placement.

- Thermal Expansion (drift). The interferometer elements and substrate are held in place by parts that will expand and contract with differences in temperature. In conventional SEBL systems, the temperature must be controlled to 1/100 ^{o}C or better, and materials with low thermal expansion coefficients are used. Furthermore, since the sample is merely fixed to the stage and is not a part of it, the measured stage position doesn't necessarily correspond to the sample position. As both objects are not made of the same material, the difference in thermal expansion coefficients can cause the sample position to drift with respect to the stage.

Intrafield Errors

Following factors contribute to intrafield errors [6]:

- Electron-optical distortions caused by abberations in the lens and deflection fields.
- Electrostatic charging of column and sample that produces spurious fields deflecting electrons from their trajectories. As the accumulated charge becomes large, the electric field may break down, removing the charge. Thus, the electron beam will slowly shift away from its intended position and suddenly jump back as spontaneous breakdown occurs. This is clearly undesirable.
- Thermal expansion and drift that cause the entire column to slowly tilt resulting in beam pointing and placement errors.
- Mechanical vibrations that couple into the electron beam column.
- Stray electro-magnetic fields that cause unwanted spurious deflection of the beam.

1.2 Spatial-Phase-Locked Electron-Beam Lithography

Imagine an archer shooting at a target. He is so skilled that he can hit bullseye every time even after he is blindfolded. Now imagine that a second target is placed 10 steps to the right of the first one. The archer, still blindfolded, is asked to take 10 steps to the right and shoot at the second target. With the addition of wind and earthquakes, this analogy gives a good picture of what is happening in a SEBL system. Here, the arrows represent electrons, wind is stray electro-magnetic fields, and earthquakes are mechanical vibrations. If the blindfold is removed, the archer has much better chance of hitting the second target. The purpose of SPLEBL is to remove this blindfold thus increasing the pattern-placement precision.

1.2.1 Overview of Spatial-Phase-Locked Electron-Beam Lithography

Large pattern-placement errors in conventional SEBL systems are mostly due to indirect referencing employed by commercial systems. The actual position of the electron beam is not known with certainty while the patterns are being written, and the beam position is inferred from the position of the substrate-holding stage. In contrast, SPLEBL employs direct referencing to achieve sub-nanometer placement accuracy. For this technique an electron-transparent fiducial grid with long-range spatial-phase coherence is patterned on the substrate prior to the e-beam exposure (Fig. 1-2). As the e-beam scans over the substrate exposing a pattern, a periodic signal is created from the interaction of the beam with the fiducial grid. The phase of this signal provides information about the e-beam position and is fed back to the beam-control electronics, which lock the electron beam to the spatial phase of the fiducial grid. Since the spatially-coherent grid is everywhere on the substrate, and since all the patterns are placed with direct referencing to this grid, the pattern-placement errors can be reduced to the 1 nm level.

1.2.2 Dose-Modulation for Spatial-Phase-Locked Electron-Beam Lithography

For maximum pattern-placement accuracy, it is essential to provide continuous feedback from the fiducial grid. If the feedback signal is interrupted at any point, the phase information encoded in it is lost. This means that there must be a periodic signal from the reference grid even when the e-beam is "turned off" and is not exposing a pattern on the substrate. This is achieved by partially blanking the beam to reduce its current by approximately an order of magnitude. The partially blanked beam does not expose the pattern because of the high non-linearity of the electron-beam-resist; yet, it can provide enough interaction with the fiducial grid to produce the periodic feedback signal. Thus, a device that can modulate the beam current by an order of magnitude at a high rate is needed. Modern commercial equipment operates at

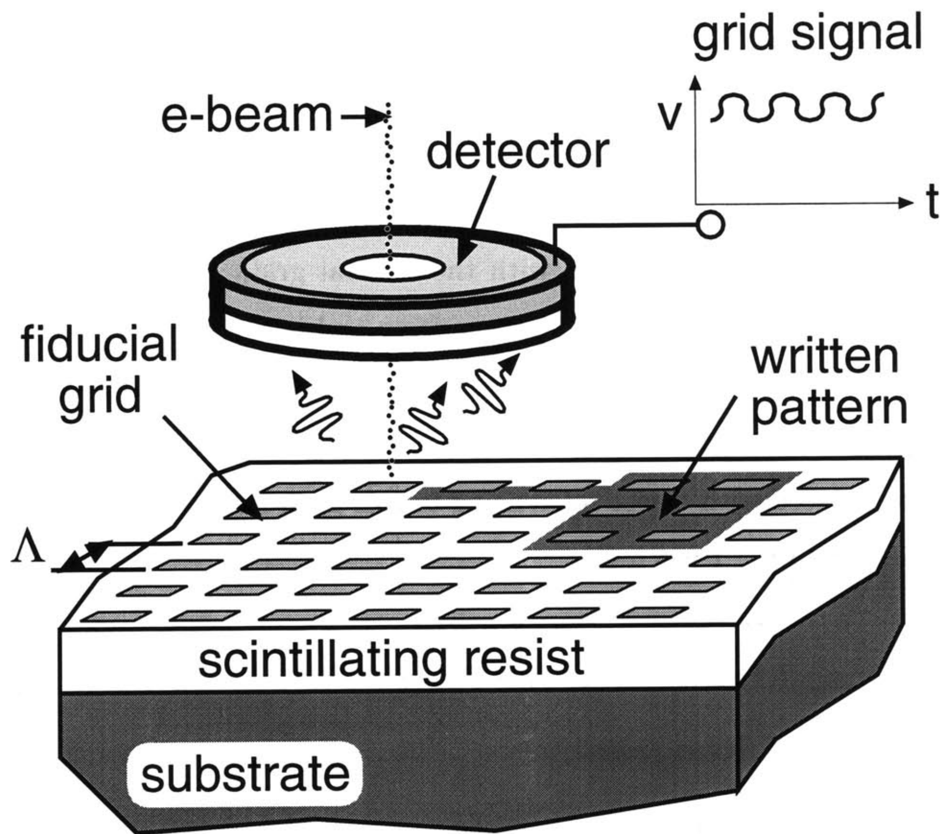

Figure 1-2: Spatial-Phase-Locked Electron-Beam Lithography

[11]

writing rates greater than 100 MHz or 10 ns per pixel exposed. Therefore, the device must be able to adjust the beam current on a nanosecond time scale.

In the following chapters a device with this characteristics will often be referred to as "dose modulator". However, a distinction must be made between modulating the beam current and the dose. Dose is the amount of energy deposited into the resist on the substrate, which is proportional to the beam current and the exposure time. Therefore, modulation of the beam current implies dose modulation assuming that exposure time per pixel remains constant. However, it is also possible to vary the dose by varying the exposure time per pixel. In the following chapter, several dose modulation schemes are described and their applicability to SPLEBL is discussed.

Chapter 2

Dose Modulation

There are several approaches to dose modulation that have been considered in this study. The schemes where exposure time instead of the beam current is varied are not suitable for use in continuously-locked SPLEBL. These schemes include beam blanking with varying duty cycle [5, 16]; and multi-pass exposure system, where dose is proportional to the number of times a pixel was exposed. In such schemes complete beam blanking is used, and the feedback signal is lost when the beam is turned off. Therefore, schemes that modulate beam current must be used. In practice, the beam current can be adjusted in two different ways. It is possible to operate on the source of electrons changing its emission properties so that fewer electrons are emitted. Alternatively, it is possible to obstruct the beam propagation, so that fewer electrons make it down the column to the substrate.

2.1 Partial Blanking

2.1.1 Magnetic Lenses

In conventional systems, the dose is modulated by a pair of magnetic lenses. The first lens is used to diverge the beam, which is then passed through a limiting aperture and focused by the second lens (Fig. 2-1). By adjusting the amount of beam divergence by the first lens it is possible to achieve arbitrary intensities. This scheme, however,

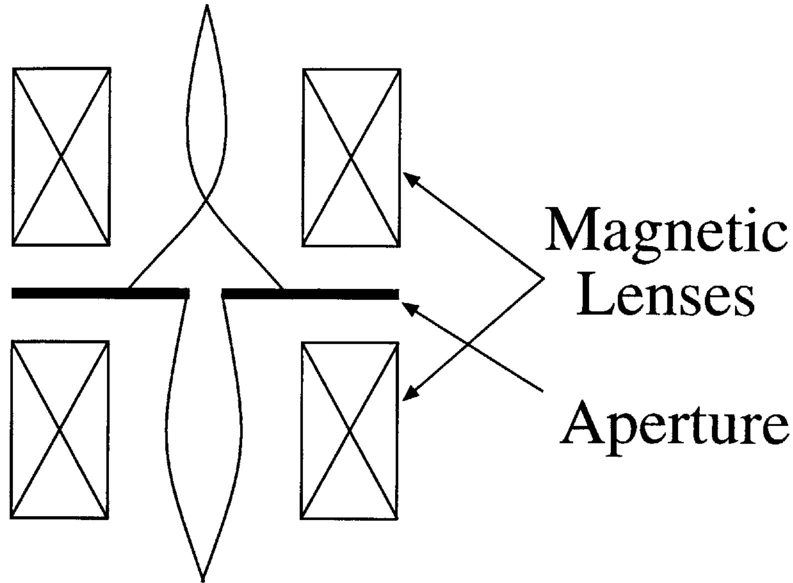

Figure 2-1: Use of Magnetic Lenses for Dose Modulation

has a slow response time due to the use of magnetic lenses. Magnetic lenses have high inductance, require high current, and thus cannot be driven at the desired high speed.

2.1.2 Conventional Blanker

Every electron beam system includes a blanker that is used to "turn off" the beam. This is accomplished by using a pair of parallel plates that create an electric field transversely oriented to the electron-beam propagation. When a potential is applied to the plates, the beam is deflected away from a beam-forming aperture and never reaches the substrate. If the deflecting voltage is lowered, the beam will be only partially deflected and some of it may pass through the beam-forming aperture. However, in this dose-modulation scheme, the image on the substrate has been observed to shift (Fig. 2-2) [10]. It is possible to correct for this shift with the deflection coils later in the column, but the amount of shift drifts with time. SPLEBL, however, depends on a constant amount of phase shift between "fully on" and "partly on" states. Thus this approach is unsuitable for use in SPLEBL.

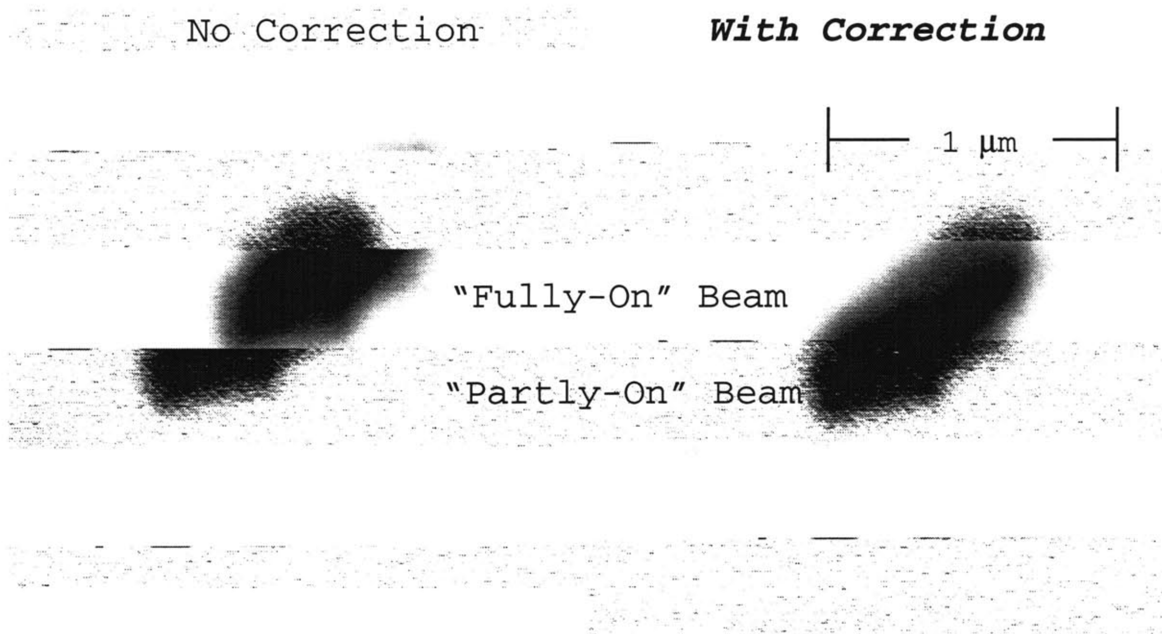

Figure 2-2: Image Shift in Conventional Blanking.

[10]

2.2 Controlling Emission

2.2.1 Thermionic Emitters

Many SEBL systems use thermionic emitters as an electron source. In a thermionic emitter, the source is heated by passing high current through it. Some thermal electrons acquire enough energy to escape the surface of the source. They are then removed away from the surface by the accelerating electric field. A Wehnelt electrode is used to control the electric field near the source surface, in such way that only some electrons are removed from the surface. By adjusting the potential applied to the Wehnelt, it is possible to control the size of the emission area, and thus control the current (Fig. 2-3). By varying the design parameters such as the size of the Wehnelt aperture and source-to-Wehnelt distance, it is possible to reduce the voltage swing required to control the beam current [4]. Although several optimized designs were investigated, these systems still require voltage swings on the order of 100 V, and, therefore, cannot be readily operated at high speeds.

2.2.2 Field Emission

Field emission sources are commonly used in electron-beam systems, since they are capable of producing much finer spot sizes than thermionic emitters. As with thermionic sources, it is possible to adjust current by varying the potential applied to the gate electrode. However, the voltage swing of hundred of volts is required to change the current by an order of magnitude. Therefore, this method of current modulation is unsuited for high speed operation. It is possible to reduce the required voltage swing by reducing the size of the tip and diameter of the gate aperture. Recently, arrays of miniature field emitters with gate diameters as small as 100 nm were fabricated [18]. While the voltage swing required to control these tips can be as small as 5 V, their emission is unstable and not suited for use in electron-beam lithography. Using arrays of such tips improves stability, but increases the source size, which is also undesirable for electron-beam lithography.

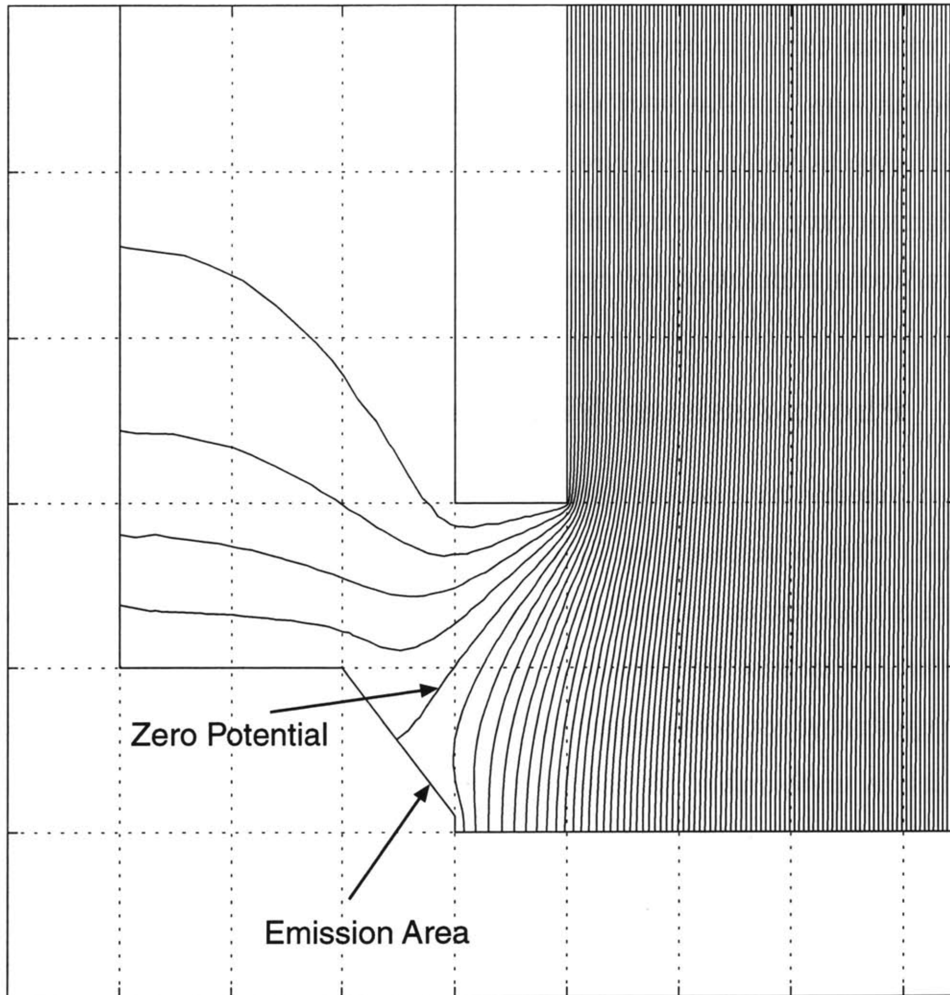

Figure 2-3: Equipotential Lines in a Thermionic Emitter.
Axially-symmetric electric fields were calculated numerically using the partial differential equation toolbox for MATLAB. Notice the zero potential line terminating on the cathode. Thermal electrons leaving the surface of the cathode to the right of this line are accelerated away from the surface and form electron beam. Emission is suppressed to the left of the zero equipotential.

2.2.3 Photo-cathodes

In recent years, different types of photo-cathodes were proposed as electron sources for lithography and other applications [2, 3, 15, 20, 21]. Such photo-cathodes can be controlled optically by a CW or pulsed laser beam. The electron-beam current is proportional to the intensity of the incident laser light. While such cathodes have many advantages, such as very short on/off transition times, they suffer from many disadvantages as well. They are highly susceptible to contamination and require ultra-high vacuum, and even then their lifetime is quite short. These problems render photo-cathodes impractical for commercial systems.

2.2.4 Photo-Assisted Field Emission

It is also possible to combine the photo-effect with a high electric field to produce electrons. This is achieved by illuminating a field emitter by a focused laser light [14]. While high extraction field increases the photo-yield when compared to regular-photoeffect, an intense light beam is required for the effect to be significant. However, the energy that is not being absorbed by photo-electrons results in the heating of the tip, which is undesirable. It has been shown that the current increase due to the increase in tip temperature dominates over photocurrent [14]. The characteristic time constant for heating and cooling process of the tip was found to be on the order of microseconds which does not meet the desired requirements for switching speed.

2.3 Electrostatic Quadra-deflector

This study proposes the use of four electrostatic deflecting plates and aperture strip to modulate the electron-beam current. The beam is deflected back and forth between two differently sized apertures that limit the beam current in proportion to their size. The basic principle of operation is illustrated in Fig. 2-4 [10]. A result of a MATLAB simulation of electron trajectories through the quadra deflector is shown in Fig. 2-5. The first two deflectors deflect the beam off-axis where it passes through a limiting

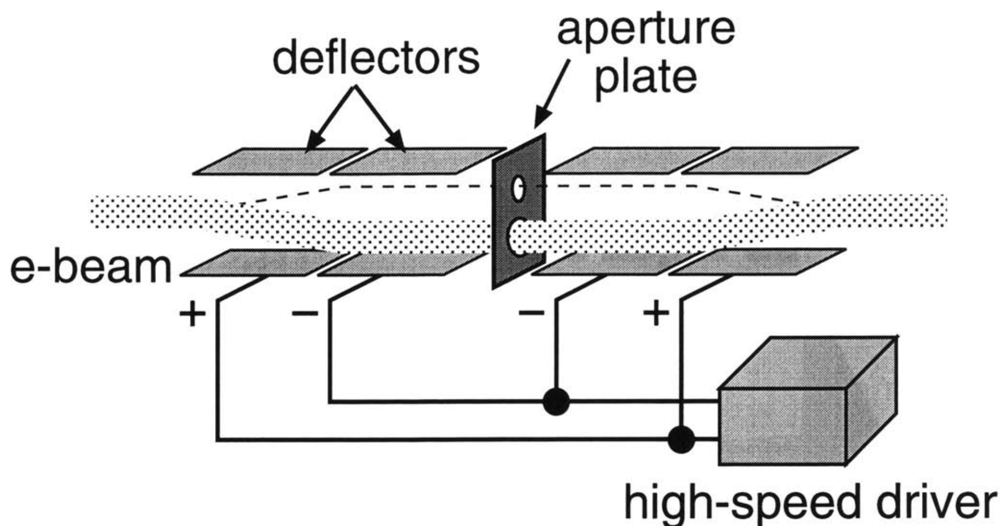

Figure 2-4: Schematic of the Quadra-Deflector

aperture. It is then returned back to the axis by the third and fourth sets of deflectors.

A similar system was implemented at the IBM T.J. Watson Research Center [13] in 1983. However, Kern *et al.* were primarily interested in varying the beam size which was only the secondary effect rather than the beam current in their system. This has led them to stop the research in this area. Also, a commercially available Zeiss SEM uses an array of differently sized apertures and magnetic deflection coils to select any aperture as needed. The use of magnetic coil, however, severely limits the maximum switching rate.

The proposed dose modulation scheme with the quadra-deflector has numerous advantages. First of all, electrostatic deflectors are widely used in conventional blanking systems and have a very fast response time. An extensive knowledge base of electrostatic deflectors has been accumulated [9, 8], and thus the design stage is greatly simplified. This scheme can also be extended to provide several different doses by using an array (more than two) of limiting apertures. It is also possible to blank the beam off completely if needed by deflecting it away from any aperture. Finally, because of high symmetry the system can be operated at high blanking rates with no spurious beam deflections due to ringing in the blanking signal. Instead of the spurious deflection, the ringing causes slight variation in the beam intensity which

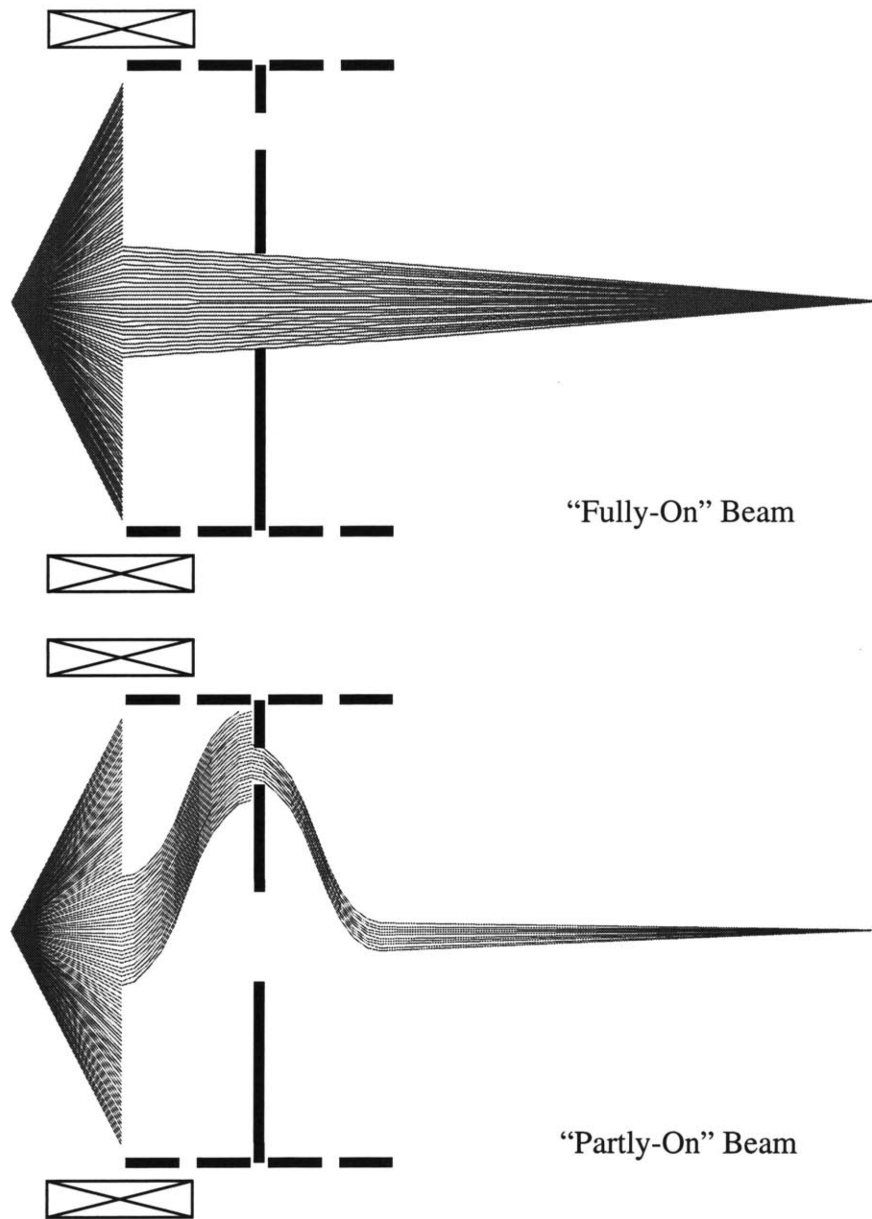

Figure 2-5: Simulation of the Operation of the Quadra Deflector

should be averaged to the true intensity over the time of exposure.

Chapter 3

Analytical Description of a Quadra-Deflector

Figure 3-1 shows the coordinates and basic geometry of a dose modulator on which all the analytical calculations in this chapter are based. Additionally, the following symbols used:

- v_z is the speed of the electrons along the z axis
- V_a is the accelerating voltage
- V is voltage applied to the deflector plates
- s is the amount of the beam deflection (shift)
- e electron charge
- m electron mass

First, the static case is considered and static deflection is found. Then, the effects of rising or falling signal on the blanker performance are analyzed.

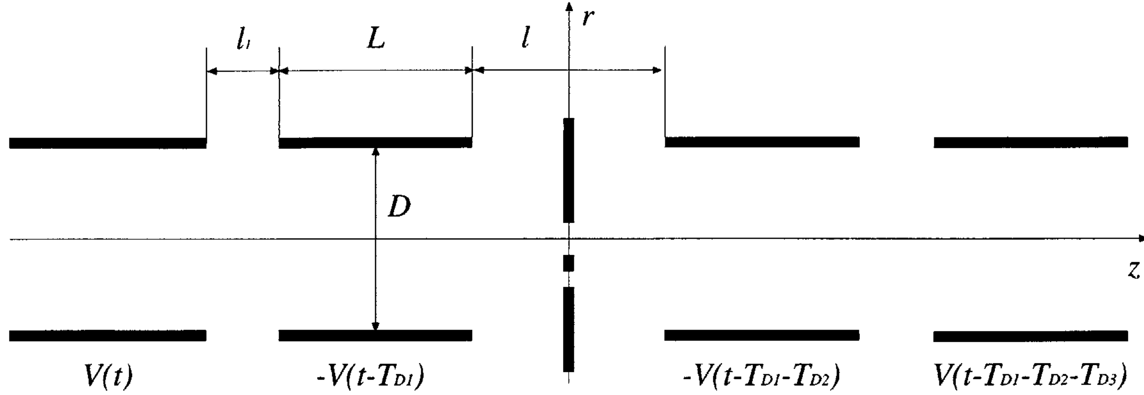

Figure 3-1: Dose Modulator Geometry
L, l, l_1, and D are the length, separations, and the gap of the deflection plates. $V(t)$ is the applied voltage. The deflecting signal doesn't have to be applied to all four deflectors simultaneously; T_{D1}, T_{D2} and T_{D3} are the time delays for application of the signal to the consecutive set of plates deflectors.

3.1 Static Deflection

3.1.1 Transverse Acceleration

While in the electric field produced by the deflector plates, electrons are subject to the transverse acceleration a which can be expressed as

$$a = \frac{F}{m} = \frac{e}{m}\frac{V}{D}$$

3.1.2 Deflection at the Aperture Strip

The time of flight through one deflector plate is determined by $T_L = L/v_z$. Similarly, the time of flight between deflectors is $T_{l1} = l_1/v_z$. Thus, the after passing through two deflectors the beam is shifted by the amount

$$s = 2\frac{aT_L{}^2}{2} + (at_L)T_{l1} = a\frac{L(L+l_1)}{v_z{}^2}$$

Substituting for a and noticing that $mv_z{}^2/2$ is the beam energy $E = eV_a$, the

following relationship is obtained

$$s = \frac{1}{2}\frac{eV}{E}\frac{L(L+l_1)}{D} = \frac{1}{2}\frac{V}{V_a}\frac{L(L+l_1)}{D}$$

3.2 Dynamic Operation

3.2.1 Writing Frequency

Two factors limit the writing frequency. The length of the blanker limits the maximum frequency of the driving signal applied to the quadra deflector, while capacitance of the blanker limits the rise and fall times.

Geometric Constraint

In order for an electron to be deflected by a full amount while passing through one of the deflectors, it must be subject to the deflecting field for that whole time. This can only happen if the blanking pulse is at least as long as the time of flight of an electron through the deflector. Therefore, the signal must be on for at least an interval of T_L. Then, for a 10 kV beam, the maximum plate length that satisfies a 1 ns switching time requirement is about 60 mm long.

Switching Time

The rise time for the modulated beam current can only be as fast as the driving signal. The rise time of the driving signal is limited by the capacitance of the deflector. If 60 mm by 20 mm plates are used with a 2 mm gap between them, the resulting capacitance would be approximately 5 pF. If the deflector is driven by a line with 50 Ω impedance, the resulting rise time is $T_R = 2.2RC$ =0.55 ns.

Maximum Writing Frequency

Therefore, the maximum writing frequency is $\approx \frac{1}{T_L+T_R}$. For the dimensions used above the resulting frequency is $\frac{1}{1+0.55}$ = 645 MHz. Thus, a quadra-deflection dose

modulator meets the established switching time requirements.

3.2.2 Delay Times

For maximum performance, time delays between signals applied to the plates need to be introduced. These delays must be chosen in such a way, that an electron flying through any of the four deflectors is always subject to the same field as it experienced in the previous deflector. This is achieved by setting, $T_{D1} = T_{D3} = T_L + T_{l1}$ and $T_{D2} = T_L + T_l$ as show show in Figure 3-1. An analytical model formulated by H. Paik it et al must be used to find the optimum time delays [17]. This is the subject of further study for optimal dynamic operation.

3.3 High-Energy Beams

Classical mechanics was used in the preceding derivations. However, electron-beam systems are often operated at beam energies of the order of 10-100 keV. At such energies the e-beam becomes mildly relativistic, and the plates are subject to relativistic length contraction. However, the same formulas still if the length of plates is replaced by their effective length $L_{eff} = L\sqrt{1 - \frac{{v_{beam}}^2}{c^2}}$.

Chapter 4

Experimental Set-up and Results

4.1 Experimental set-up

The general view of the experimental set-up is shown in Figure 4-1. The setup consists of vacuum chamber that houses electron source, dose modulator, and other electron-optical components.

4.1.1 Vacuum System

The vacuum chamber was built from three 8-inch ConFlat flange pipe segments. On one end it was capped with a glass viewport, while the other end was capped with a high-voltage electrical feedthrough that was used to power up an electron source. A turbo pump backed by a mechanical pump was used to rough the chamber to approximately 10^{-4} torr. At this point a Varian Triode $400l/s$ ion pump was started and a base pressure of 10^{-7}-10^{-8} torr was reached. The chamber volume was $\approx$0.7 m^3, and the pump-down time to 10^{-7} was 24 hours. An overnight bake at 100 ^{o}C was required to reach 10^{-8} torr.

4.1.2 Electron-Optical Rail

A long aluminum rail with V-shaped groove was used to mount components inside the vacuum chamber. The V-shaped grove allows aligned placement of cylindrical

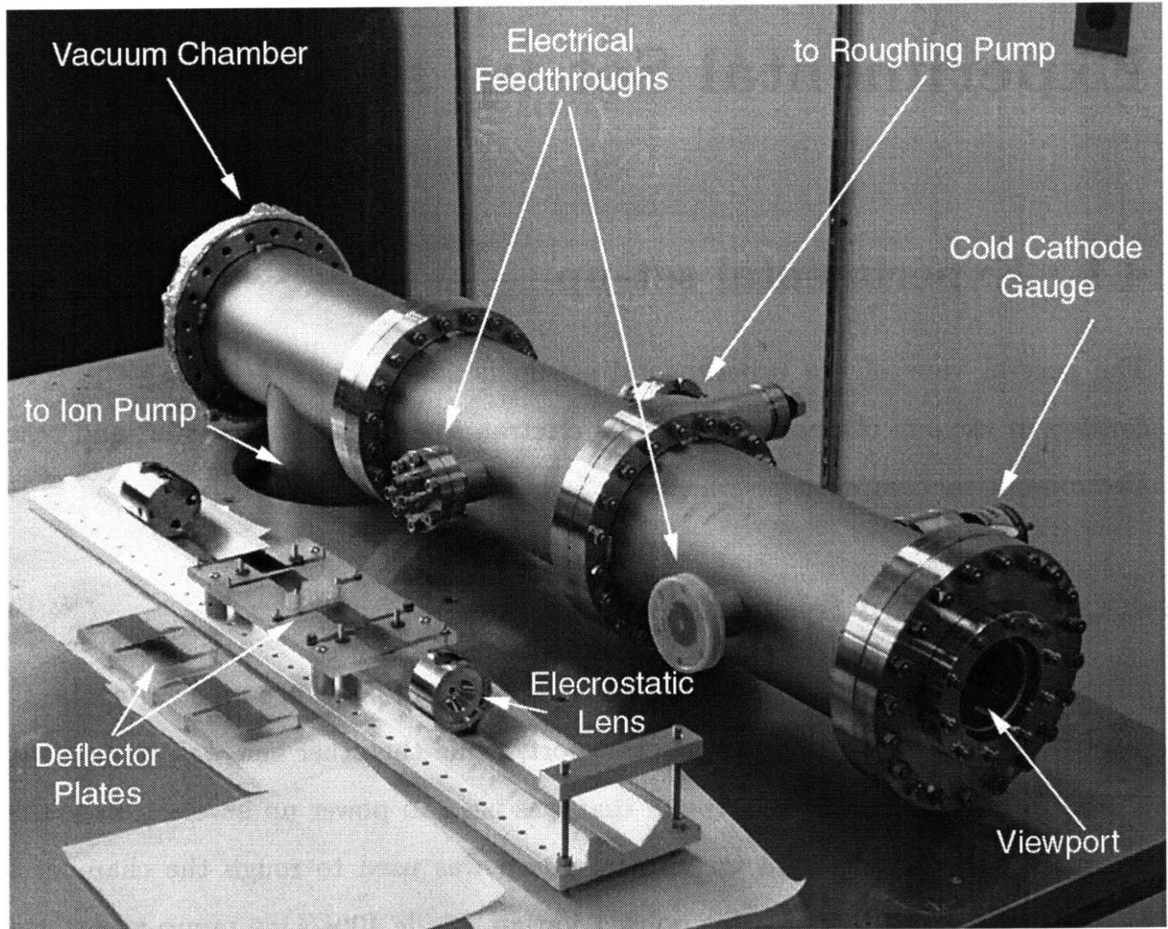

Figure 4-1: Experimental Setup

components such as electrostatic lenses [22, 19]. Along the edge of the rail are 1-inch space 1/4-20 holes which are used to mount additional components such as apertures and deflection plates.

4.1.3 Electrostatic Einzel Lenses

Electrostatic Einzel lenses were obtained on loan from Portland State University to produce an image of the source. The lenses were designed by Prof. G. Rempfer [19]. Their focal length can be adjusted by applying potential difference between the center electrode and the grounded outer electrodes. For the type of lenses that we had, 0-3 kV adjustment results in the focal length changing from infinity to approximately 3 inches.

4.1.4 Electron Source

For initial experiments an array of silicon field emission tips fabricated at MIT was used as the source. Despite several attempts, emission was not obtained from the source. This was, most likely, the result of the emitting surface contamination by oil from the mechanical and turbo pumps.

Subsequently, a tungsten hairpin emitter was used as an electron source (Fig. 4-2). It was positioned in front of the .024 inch aperture that acted as a Wehnelt. A Bertan E-50B power supply was used to supply filament current and beam accelerating voltage. The emission properties of the resulting electron gun are shown in Figure 4-3. Due to the type of electrical feedthrough used, the beam voltage was limited to 3 kV.

4.1.5 Blanking Assembly

Deflector Plates

The deflector plates were fabricated by evaporating a thin layer of gold through a stencil mask on a flat piece of Rexolite plastic. Rexolite has low out-gassing rate which makes it suitable for use in high-vacuum applications. The gap between two such plates was set by spacers. The plates were designed for use with 10 kV beam,

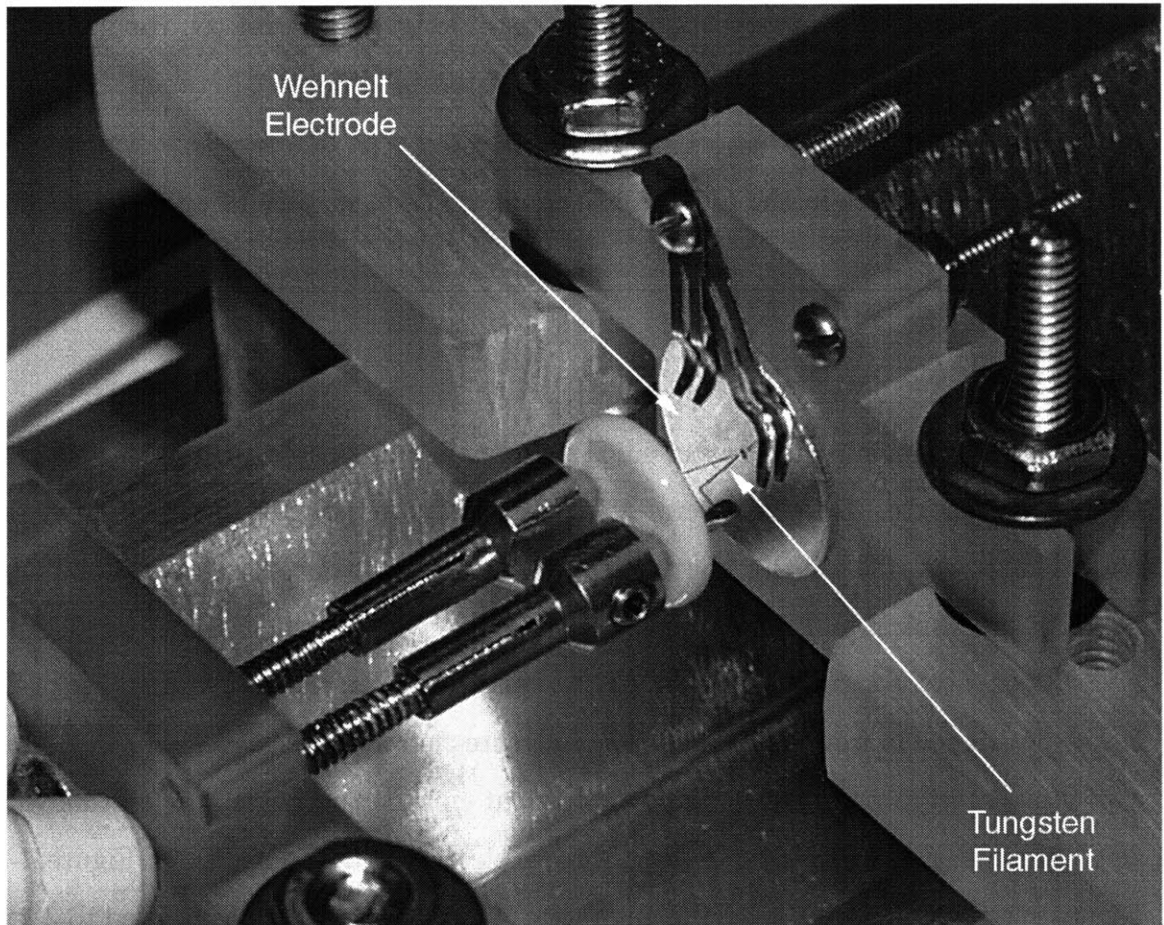

Figure 4-2: Tungsten Hairpin Electron Source

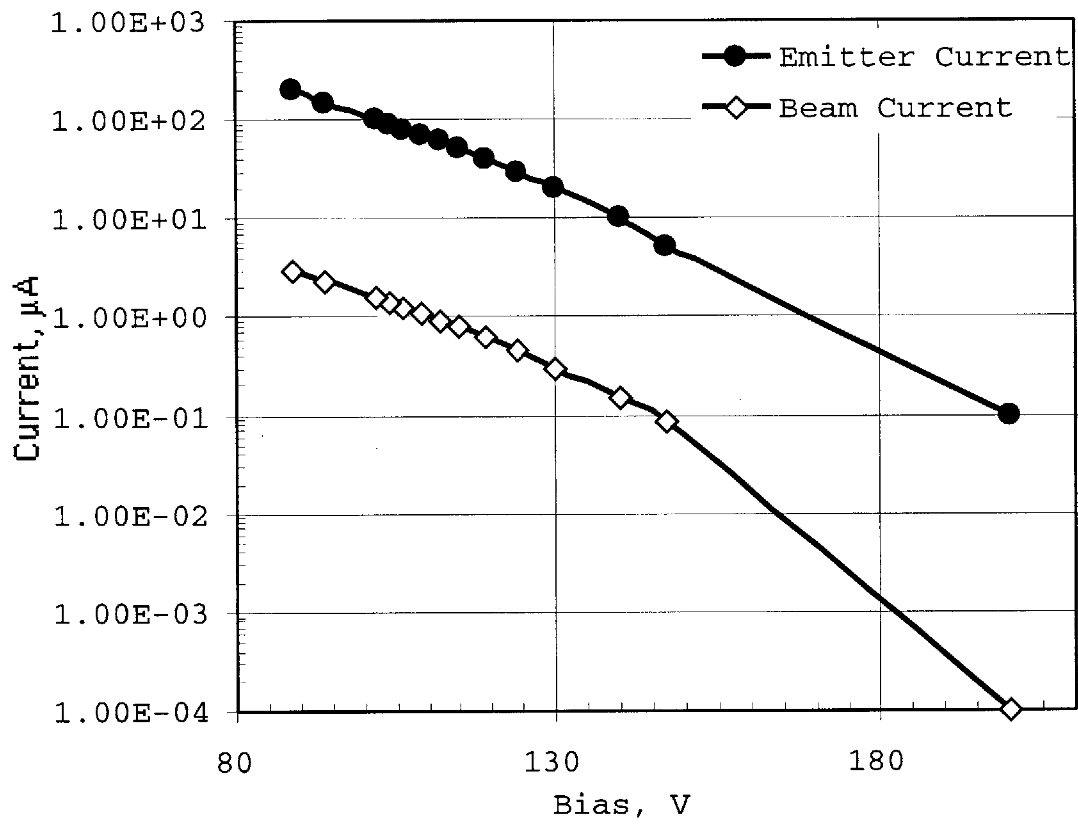

Figure 4-3: Emission Properties of Tungsten Hairpin

Plate Length, L	50 mm
Plate Width	20 mm
Gap, D	2 mm
Separation, l	29 mm
Separation, l_1	4 mm

Table 4.1: Deflector Plate Dimensions

and their dimensions were chosen in accordance with the switching rate constraints discussed in Chapter 3. The plate dimensions used are shown in Table 4.1.

Aperture Array

Given the plate dimensions used, a 10 kV beam should be deflected by approximately 350 μm by 5 V deflecting voltage. Therefore, the larger aperture size was chosen to be 300 μm, the smaller one 60 μm, and the distance between the two 300 μm.

4.2 Experimental Results

First, the switching time of the deflector plates was verified. The plates assembly was connected to the high frequency generator, and the rise time was measured. The results of this experiment are shown in Figure 4-4. The measured rise time was 6 ns which was limited by the 5 ns rise time of the driver. We expect that with a better current driver, rise times of below 1 ns can be achieved.

Then the dose modulation was observed. For this simple experiment, no lenses were used to focus the electron beam, thus resulting in a beam wide enough to cover both apertures. As the deflecting voltage was applied to the plates, the beam shifted. Because of the Gaussian-beam intensity profile, a change in the beam intensity passing through the apertures resulted. A wide metal plate was used as the detector; the beam current was measured as the current between this plate and the ground. The results of this experiment are shown in the Figure 4-5 below. Sharp spikes observed are due to proximity of the detector plate plate to the deflectors. These could be reduced by moving the detector away from the the deflectors' fronging fields. The slow rise and

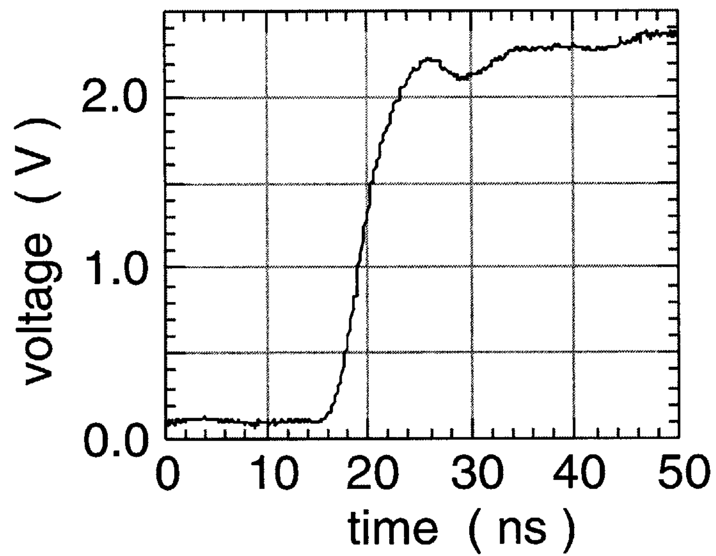

Figure 4-4: Deflector Plates Switching Rate.
The rise time was limited by the rise time of the driving signal. With a better current driver, rise time shorter than 1 ns is anticipated.

fall times, $\approx$ 100 ms, were most likely caused by the charging of Rexolite. As the beam shifted from one position to another, the charge distribution changed as well. This effect could be reduced by replacing metal-on-plastic plates by purely metal plates.

Finally, an additional limiting aperture was installed into the system. This apertured limited the beam size in the aperture array plane to approximately 300 μm. Also, a metal plate was replaced by a solid state detector. Unfortunately, no beam current was observed in this second experiment. This was either due to problems in the source to apertures alignment; or due to low energy 3 kV electrons not being able to penetrate into the active region of the solid state detector.

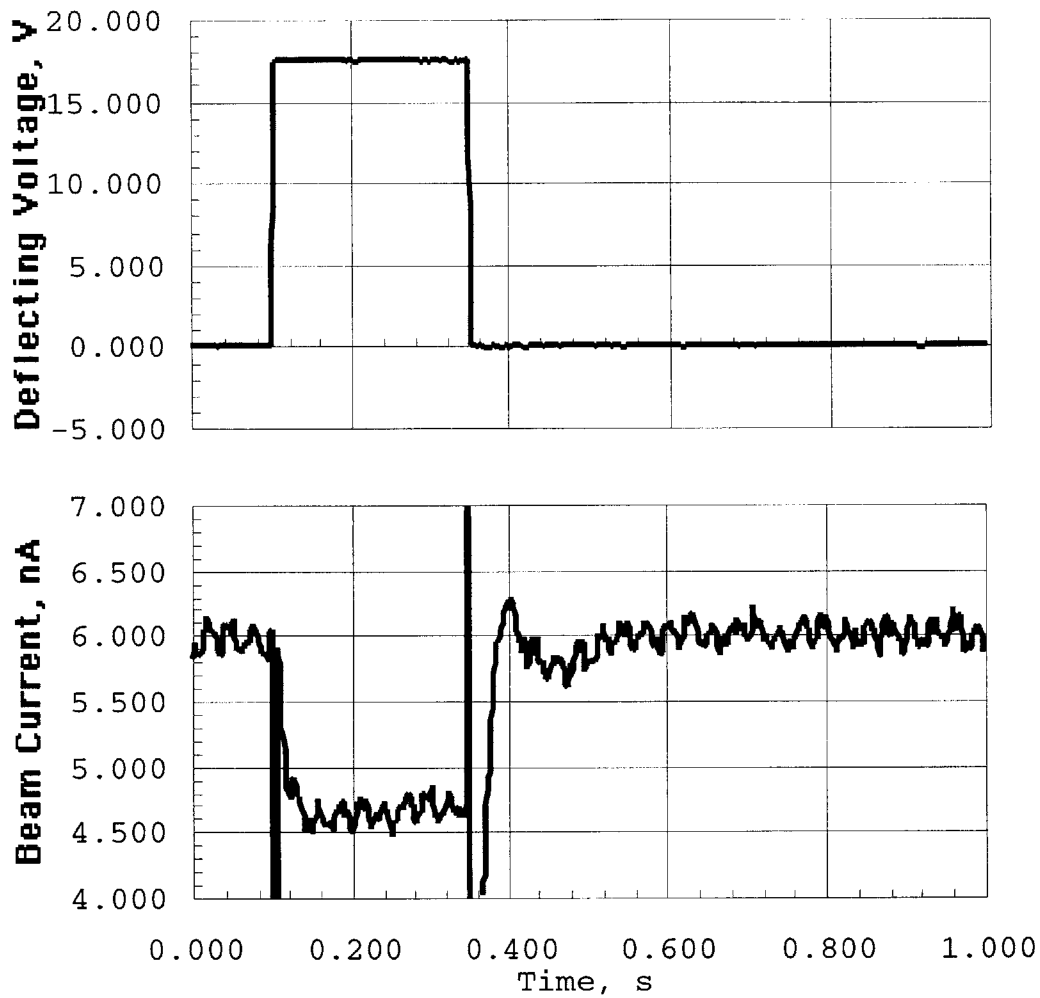

Figure 4-5: Intensity Modulation in a Wide Beam.
Sharp spikes seen here are the result of undesirable crosstalk between the wires driving the deflector plates and the beam detector wires. Slow rise and fall times are most likely caused by the parasitic capacitances of metal detector plate and inductance of detector wires.

Chapter 5

Conclusion

The problem of the beam current modulation has been addressed by the work described in this thesis. Specifically, a new type of blanking device employing four pairs of deflector plates has been proposed.

Analytical description of the dose modulator has been given and key relationships for its optimum operation were found. Preliminary experiments to evaluate blanking performance of such a device were performed and yielded promising results.

Further testing is required to better characterize the dose modulator's performance. Specifically:

- Dose modulation by an order of magnitude must be demonstrated.
- The effect of time delays on dose modulator's performance needs to be measured and compared with analytical findings.
- Absence of the image shift has to be demonstrated.
- Finally, a dose modulator needs to be integrated into an existing electron-beam system, and continuous spatial-phase-locking needs to be demonstrated.

The deflection scheme proposed here can be further developed and used in applications other than SPLEBL. Some of this developments and uses are:

1. Multiple Doses. By using an array of differently sized apertures more than two

different doses can be produced. This could be useful for gray-beam writing strategies [1].

2. Complete Beam Blanking. This deflection scheme can be used to provide complete blanking without spurious beam deflection. Spurious beam deflection is one of the problems that limits the speed of an electron beam system.

3. Proximity Effect Correction. High-speed dose modulation also enables write-time proximity-effect corrections, via the GHOST method, and improved line width control. Thus a high-speed dose modulator can also be used to enhance the patterning capability of conventional SEBL systems.

Pattern placement requirements constitute a significant obstacle in the development of future fabrication technologies, which will produce higher device densities then those available today. SPLEBL, with the dose modulation scheme presented here, may be a solution to this problem.

Bibliography

[1] F. Abboud, R. Dean, J. Doering, M. Gesley, U. Hoffman, T. Mullera, R. Nabber, M. Pastor, W. Phillips, J. Raphael, F. Raymond III, and C. Sauer. Multipass gray prinitng for new MEBES 4500S mask lithography system. In *Photomask and X-Ray Mask Technolgy IV*, volume 3096, pages 116–124, Kawasaki, Japan, 1997.

[2] A. Aboubacar, M. Dupont, J. Gardes, M. Laguna, M. Querrou, and L.P Says. Electron beams triggered by a laser pulse of a few tens ns duration from silicon cathodes with array of tips in high electric field. *Nuclear Instruments and Methods in Physics Research A*, 340:74–79, 1994.

[3] Marco Batinic, Dietmar Begert, and Erich Kubalek. Pulsed electron beam generation via laser stimulation. *Nuclear Instruments and Methods in Physics Resarch A*, 363:43–47, 1995.

[4] S.M. Davidson. Wehnelt modulation beam blanking in the scanning electron microscope. In M.J. Goringe, editor, *Proceedings of the Institute of Physics Electron Microscopy and Analysis Group Conference*, pages 39–42, Cambridge, UK, 1982. IOP; Bristol, UK.

[5] J. Fehr, W. Reiners, L.J. Balk, E. Kubalek, D. Kother, and I. Wolff. A 100-femtosecond electron beam blanking system. *Microelectronic Engineering*, 12:221–26, 1990.

[6] J. Ferrera. Highly coherent gratings for optoelectronics: An application of spatial-phase-locked electron beam lithography. Master's thesis, Massachusetts Institute of Technology, 1994.

[7] J. Ferrera, V.V. Wong, S. Rishton, V. Boegli, E.H. Anderson, D.P. Kern, and H.I. Smith. Spatial-phase-locked electron-beam lithography: Initial test results. *J. Vac Sci. Technol. B*, 11:2342–5, 1993.

[8] M. Gesley, D. Colby, F. Raymond, D. McClure, and F. Abboud. Electrodynamics of fast beam blankers. *J. Vac Sci. Technol. B*, 11(6):2378–85, 1993.

[9] Mark Gesley and Pat Condran. Electron beam blanker optics. *J. Vac Sci. Technol. B*, 8(6):1666–72, 1990.

[10] J. Goodberlet. Private communication, 1999.

[11] J. Goodberlet, J. Ferrera, and Henry I. Smith. Spatial-phase-locked electron-beam lithography with a delay locked loop. *J. Vac Sci. Technol. B*, 15(6):2293–97, 1997.

[12] J. Goodberlet, S. Silverman, J. Ferrera, M. Mondol, M.L. Schattenburg, and H.I. Smith. A one-dimensional demonstration of spatial-phase-locked electron-beam lithography. *Microelectronic Engineering*, 5:473–476, 1997.

[13] D.P. Kern, R. Viswanathan, R.H. Naumann, and T.H.P. Chang. A round beam exposure system with multiple beam sizes. In *Proc. 10th International Conference on Electron and Ion Beam Science and Technology*, pages 15–27, Quebec, 1983. Electrochemical Society.

[14] M. J. G. Lee and E.S. Robins. Thermal relaxation of a laser illuminated field emitter. *J. Apple Phys*, 65(4):1699–1706, February 1989.

[15] Gail A. Massey, Steben E. Bowersox, Saeid Ghamaty, and Ali Rahbar. Nonlinear photoemisson from organic cathodes excited by a pulsed near-ultraviolet laser. *IEEE Journal of Quantum Electronics*, 23(12):2054–59, December 1987.

[16] Andrew Muray, Dave Colby, Robin Teitzel, and Mark Gesley. Experimental evaluation of an electron-beam pulse modulated blanker (160 mhz) for next-generation electron-beam raster scan systems. *J. Vac Sci. Technol. B*, 13(6):2488–92, 1995.

[17] H. Paik, E. Kirklnad, and B.M. Siegel. Analytical calculation of electrostatic beam blanker preformance. *Journal of Physics E (Scientific Instruments)*, 20(1):61–66, January 1987.

[18] David G. Pflug, Mark Schattenburg, Henry I. Smith, and Akintunde I. Akinwande. 100nm gate aperture field emitter arrays. In *International Vacuum MicroElectronics Conference*, 1998.

[19] Gertrude F. Rempfer. Unipotential electrostatic lenses: paraxial properties and aberrations of focal length and focal point. *J. Appl. Phys*, 57(7):2385–2401, April 1985.

[20] Colin A. Sanford and Noel C. MacDonald. High speed e-beam testing using GaAs negative electron affinity photocathodes. *Microelectronic Enginnering*, 12:213–20, 1990.

[21] J. E. Schneider, A. W. Baum, G. I. Winograd, R. F. W. Pease, and M. McCord. Semiconductor on glass photocathodes as high-performance sources of parallel electron beam lithography. *J. Vac. Sci Technol. B*, 14(6):3782–3786, 1996.

[22] Walter P. Skoczylas, Gertrude F. Rempfer, and O. Hayes Griffith. Electron optical benches for in-line and branched systems. a new bench designed for mirror based aberration correction and low energy electron microscopy. *Rev. Sci. Instrum*, 65(10):3183+, October 1994.